Structure and Dynamics of the Sialic Acid Moiety of G_{M3}-Ganglioside at the Surface of a Magnetically Oriented Membrane†

Yves Aubin,‡ Yukishige Ito,§ James C. Paulson,‖ and James H. Prestegard*,‡

Department of Chemistry, Yale University, New Haven, Connecticut 06511, and Cytel Corporation, 3525 John Hopkins Court, San Diego, California 92121

Received July 13, 1993; Revised Manuscript Received October 6, 1993⊛

ABSTRACT: ^{13}C-NMR techniques in oriented bilayer systems composed of DMPC and CHAPSO have been used to measure dipolar interactions between ^{13}C–^{13}C and ^{13}C–^{1}H pairs located in the sialic acid moiety of ganglioside G_{M3}. These interactions are reduced to a structural and motional model for the headgroup of this glycolipid using an order matrix approach. The analysis shows an average structure possessing a high degree of order and is most consistent with structures that are well extended from the membrane surface. Saturation of the ganglioside environment with high concentrations of Ca^{2+} (0.28 M) produces a small perturbation of the headgroup. G_{M3} dissolved in a DMPC/CHAPSO system can also be demonstrated to bind wheat germ agglutinin (WGA). The minimal perturbation of structure-dependent parameters suggests that the dominant structure of the sialic acid moiety in the isolated membrane system is favored for binding by the protein.

There has been considerable interest in the structural characterization of glycoconjugates which act as membrane surface receptors for proteins involved in physiological and pathological processes (Lasky, 1992; Sharon & Halina, 1993). Recently we, and others, have undertaken a program to develop NMR methods for the study of the carbohydrate portion of these molecules in an environment which approximates their membrane-like natural state (Frenske *et al.*, 1991; Aubin & Prestegard, 1993). Our application of these methods have so far been to rather simple glycolipids or analogs of glycolipids containing a single sugar substituent. Here, we extend this work to a more complex sialic acid containing glycolipid, the ganglioside G_{M3}.

G_{M3} is a cerebroside having a nonbranched three-sugar headgroup: NeuAc-α-(2,3)-Gal-β(1,4)-Glc. At the teminus of this headgroup is an *N*-acetylneuraminic acid. This residue commonly referred to as sialic acid, is a unique monosaccharide found at the nonreducing end of the carbohydrate groups of many glycoproteins and at the headgroup terminus of many other glycosphingolipids (Rosenberg & Schengrund, 1976; Schauer, 1983). Its terminal position and its ionizable carboxyl group enables sialic acid to bind cationic cofactors and participate in a number of biological processes at the membrane surface.

Gangliosides are an important class of sialylated glycosphingolipids which are almost exclusively located at the outer leaflet of the plasma membrane. Several observations (Wiegandt, 1985; Iwamori & Nagai, 1978) have suggested that they could be involved in two basic cellular functions: (1) cell adhesion and recognition and (2) regulation and maintenance of cell growth. Both functions are greatly perturbed upon oncogenic transformation (Hakomori, 1981; Hakomori & Kannagi, 1983). Accumulating evidence suggests that the lack of contact inhibition and regulation of cell proliferation characterizing tumor cells are a result of an altered expression and organization of their gangliosides due to defective biosynthesis machinery. Any transformation that influences the activity and/or the regulation of enzymes responsible for ganglioside synthesis (glycosyl and sialyl transferase) results in an accumulation of precursors (e.g. G_{M3}, G_{D3}, G_{M2}, etc) and depletion of higher gangliosides (G_{M1}, G_{D1a}, G_{T1b}, etc.). Among the gangliosides expressed by malignant cells, G_{M3} has been the focus of many studies that suggest its direct involvement in a number of events characterizing malignancy.

Hakomori *et al.* have shown that G_{M3} modulates cell growth by inhibiting EGF-dependent tyrosine phosphorylation of the EGF-receptor in A431 and KB cells (Hannai *et al.*, 1988). They proposed that G_{M3} at the outer leaflet of the plasma membrane interacts with the receptor in such a way as to prevent the receptor aggregation needed for signal transduction through the membrane (Hannai *et al.*, 1988; Song *et al.*, 1991). Another involvement of G_{M3} in cell growth was found in the case of unregulated proliferation of melanoma B16 cells (Ravindranath *et al.*, 1989; Grayson & Ladisch, 1992). These cells are known to shed a considerable amount of membrane material containing a high concentration of G_{M3}. This appears to generate a negative immune response resulting in the enhancement of melanoma growth. A G_{M3}-antibody interaction was identified as being the major factor responsible for the negative response.

G_{M3} is also known to interact with proteins which are more readily available and better characterized structurally. These may serve as suitable models for the study of changes in the structure and dynamics of receptor headgroups on protein binding. Wheat germ agglutinin, a plant lectin, is one such protein. It is known to aggregate vesicles containing a number of derivatives of G_{M3}, and a high-resolution structure has been determined by X-ray crystallography (Wright, 1990). In fact,

† This work was supported by National Institutes of Health Grants GM33225 and GM27904. Y.A. acknowledges the support of the Ministère de l'Éducation du Québec.

* To whom correspondence should be addressed.

‡ Department of Chemistry, Yale University.

§ Current address: The Institute of Physical and Chemical Research (RIKEN), 2-1 Hirosawa, Wako-Shi, Saitma, 351-01, Japan.

‖ Cytel Corp.

⊛ Abstract published in *Advance ACS Abstracts,* November 15, 1993.

[1] Abbreviations: CHAPSO, 3-((cholamidopropyl)dimethylammonio)-2-hydroxy-1-propanesulfonate; CSA, chemical shift anisotropy; DMPC L-α-dimyristoylphosphatidylcholine; G_{M3}, NeuAcα2-3Galβ1-4Glcβ1-1Cer; NMR, nuclear magnetic resonance; NOE, nuclear Overhauser effect; WGA, wheat germ agglutinin.

0006-2960/93/0432-13405$04.00/0

the crystal structure has the headgroup of G_{M3} in its binding site. In addition to data on the structure and dynamics of a membrane-bound G_{M3} molecule, we will present here some preliminary data on the perturbation of G_{M3} upon WGA interaction.

High-resolution NMR techniques have previously been used to determine the three-dimensional structure of the headgroup of G_{M3} in solution and in a micellar environment (Siebert *et al.*, 1992; Koerner *et al.*, 1983). Here, spin relaxation interactions modulated by isotropically tumbling molecules provide the primary source of information. The studies certainly provide insight into the structure and dynamics of the headgroup, but conclusions are potentially difficult to extrapolate beyond the environment where the experiments are carried out. The methods employed here are fundamentally different in that they rely on direct measurement of dipolar splittings that are normally averaged to zero in high-resolution NMR, and they are applied to molecules embedded in more extended membrane-like fragments. The methods are more akin to solid NMR techniques except that field-oriented liquid crystals rather than randomly oriented microcrystals are used. The liquid crystals are composed of an aqueous dispersion of a 3:1 mixture of L-α-dimyristoylphosphatidylcholine (DMPC) and 3-((cholamidopropyl)dimethylammonio)-2-hydroxy-1-propanesulfonate (CHAPSO). The mixture is believed to exist as discoidal particles in which the lipid bilayer forming DMPC dominates the facial surfaces. Glycolipids anchored to these surfaces should experience an environment which approximates that of a lipid bilayer (Sanders & Prestegard, 1990). The spectroscopic methodology has been described in early papers by Sanders and Prestegard (Sanders & Prestegard, 1991, 1992).

Briefly, a rigid molecular fragment labeled with pairs of spin $^1/_2$ nuclei, and sampling on a rapid time scale an anisotropic distribution of orientations, will show splittings in high-resolution spectra arising from the dipolar interaction. The magnitude and sign will be related to the average orientation and amplitude of motion for the fragment. More formally, the dipolar interaction can be expressed in terms of an order parameter, a set of fixed nuclear properties (γ), and an internuclear distance (r) as follows:

$$D_{ij} = -\frac{h\gamma_i\gamma_j}{2\pi^2 r^3} S_{bilayer} S_{mol} \quad (1)$$

We choose to break the more conventional single-order parameter (S) into two parts, where S_{mol} is defined as

$$S_{mol} = \cos^2\phi_x(-S_{yy} - S_{zz}) + \cos^2\phi_y(S_{yy}) + \cos^2\phi_z(S_{zz}) + 2\cos\phi_x\cos\phi_y(S_{xy}) + 2\cos\phi_x\cos\phi_z(S_{xz}) + 2\cos\phi_y\cos\phi_z(S_{yz})$$

The $\cos\phi_i$ terms relate vectors connecting pairs of spins to the axes of an order tensor defined in an arbitrary molecular frame. The S_{ij} are elements of this tensor. A FORTRAN program, ORDERTEN (Sanders & Prestegard, 1991, 1992), is used to execute a systematic search of the order tensor elements to find sets of these elements that reproduce the dipolar couplings measured from the NMR spectra. After diagonalization of the order tensor, three eigenvalues are obtained as principal order tensor elements, S_{XX}, S_{YY}, and S_{ZZ}, and three eigenvectors are obtained. These describe the degree of order and the average orientation of the fragment relative to a bilayer normal respectively. $S_{bilayer}$ is experimentally determined and describes the orientation and order of the bilayer normal relative to the applied magnetic field.

The chemical shifts of ^{13}C sites in many functional groups are dependent on the structural and motional properties of molecules in which they are found. In the case of a ^{13}C-labeled sialic acid group the carbon at the anomeric carboxylate is likely to display the larger effects and these effects are expected to be orientationally dependent through the anisotropy of a chemical shift tensor. A suitable orientation and magnitude of a chemical shift tensor for the carboxylate group can be taken from the work of Pines *et al.* (Pines *et al.*, 1974). In nonisotropically averaged settings chemical shifts depend on order parameters in much the same fashion as the dipolar couplings. Thus, chemical shift can be predicted from the order tensor results above, providing confirmatory data on the analysis.

The use of ^{13}C-labeled analogs has been critical to the application of these methods. First, it provides a means of distinguishing signals of the glycolipids of interest from lipids of the liquid crystal matrix. And second, the dispersion of ^{13}C chemical shifts have been important in resolving and assigning a sufficient number of dipolar splittings to extract the five independent elements of the order tensor.

Most recently the methods were applied to a sialic acid-containing model glycolipid, α-dodecyl sialyloside. ^{13}C labels were introduced at the C_1, C_2, and C_3 on the sialic acid moiety (Aubin & Prestegard, 1993). Interaction among these three sites and the two protons attached to the C_3 carbon, in principle, can provide enough data for structure determination. Our goal was to apply the same method to structural analysis of larger glycolipids containing ^{13}C-labeled sialic acid such as G_{M3}. Although this represents a synthetic challenge, combined chemical and enzymatic approaches have made possible the synthesis of more complex carbohydrates in preparative amounts (see Ichikawa *et al.*, 1992 for a review). In particular, a synthesis of G_{M3}-ganglioside using a combination of enzymatic and chemical steps has been achieved (Ito & Paulson, 1993) with a high level of sialic acid incorporation (37%). These advances led to the study of the ^{13}C-labeled G_{M3}-ganglioside presented here.

MATERIALS AND METHODS

DMPC, CHAPSO, *N*-acetyl-D-mannosamine, *N*-acetylneuraminic acid aldolase (EC 4.1.3.3), and wheat germ agglutinin were purchased from Sigma (St. Louis, MO). Pyruvic acid (sodium salt), ^{13}C-labeled at C_1, C_2, and C_3 (99%), was purchased from MSD Isotopes (Montréal, Canada).

[1,2,3-^{13}C]-N-Acetylneuraminic Acid (α-2-3)-Lactosylceramide (G_{M3}). [1,2,3-^{13}C]-*N*-Acetylneuraminic acid (sialic acid) (*ca.* 60 mg), prepared as described elsewhere (Aubin & Prestegard, 1993), was used in the procedure reported by Ito and Paulson (Ito & Paulson, 1993) for the synthesis of 55 mg (32%) of [^{13}C]G_{M3}.

Preparation of NMR Samples and NMR Spectroscopy. In non protein containing samples, 10 mg of labeled G_{M3} was dissolved in a liquid crystal preparation consisting of a mixture of 149 mg of DMPC/CHAPSO (3:1) in 0.300 mL of phosphate buffer (50 mM in D_2O, pH 7.0). For studies with WGA, 2 mg of G_{M3} were dissolved along with 12 mg of the protein using Tris-HCl buffer (50 mM, pH 7.4) with NaCl (0.1M) and $CaCl_2$ (0.01 M). This amount of protein corresponds to near close packing of WGA molecules at full saturation of binding sites. Sample preparation involves a good deal of homogenization through cooling and warming cycles along with centrifugation. In the case of WGA-

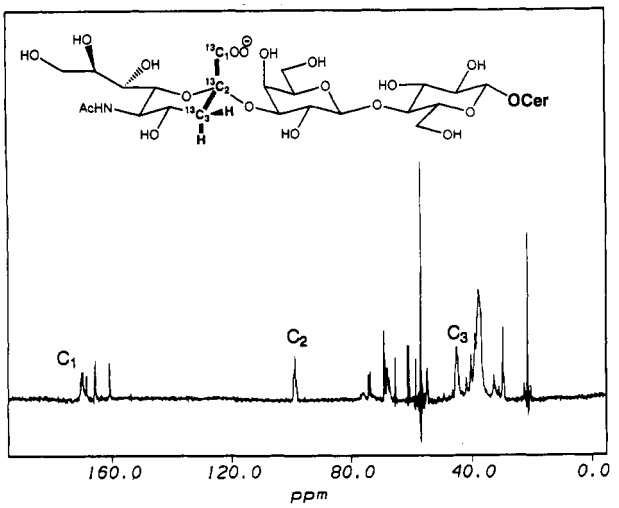

FIGURE 1: ^{1}H-decoupled inverse-gated ^{13}C-NMR spectrum (125.67 MHz) of G_{M3} ^{13}C-labeled at C_1, C_2, and C_3 of the sialic acid moiety at 99% dissolved in a DMPC/CHAPSO 3:1 at 35% (w/w) lipid content in phosphate buffer at pH 7.0 recorded at 40 °C. A Gaussian multiplication with a line-broadening factor of −1.0 Hz and a Gaussian broadening factor of 0.4 was applied prior to Fourier transform. The spectrum was referenced to the choline peak at 53 ppm.

containing samples, most of this was carried out prior to addition of WGA and glycolipid.

NMR spectroscopy as applied to structural analysis was described in detail elsewhere (Aubin & Prestegard, 1993). Briefly, ^{13}C-NMR spectra were acquired on a Bruker AM-500 spectrometer operating at 125.67 MHz. Proton homonuclear and heteronuclear decoupling were achieved using WALTZ-16 and MREV-8 composite pulse sequences, respectively, at a decoupler power of 40 W. The acquisition time was kept short (74 ms) and the relaxation time long (2 s) in order to avoid heating of the sample by the decoupler. For the variable temperature experiments, the sample in the magnet was equilibrated at a given temperature for a period of at least 20 min prior to acquisition of the spectrum. INADEQUATE spectra based on the pulse sequence of Bax and co-workers (Bax *et al.*, 1981) were employed to recover glycolipid signals from regions of the spectra obscured by background from the lipid matrix. In a number of cases, it was necessary to fit experimental line shapes to theoretical curves in order to extract coupling information. For one-dimensional multiplets, data were fit to a sum of lorentzian lines using FIT which is a program written in FORTRAN that employed a simplex algorithm (Tirado-Rives, personal communication). For INADEQUATE spectra, intensities, phases, and positions of lines were simulated with a density matrix based simulation program written in C (J. Tolman and J. H. Prestegard, manuscript in preparation).

RESULTS

Measurement of Dipolar Couplings. Figure 1 shows an inverse gated ^{1}H-decoupled ^{13}C-NMR spectrum of G_{M3} dissolved in DMPC/CHAPSO at 40 °C. The chemical shifts of the three labeled carbons, namely, C_1, C_2, and C_3, are 174, 100, and 40 ppm, respectively. The remaining peaks are from natural abundance ^{13}C carbons in the lipid matrix of the oriented liquid crystal. Three ^{13}C–^{13}C couplings can be directly measured from the C_1 and C_2 resonances which appear as doublets of doublets (see Figure 2). Since the values of the couplings are not drastically different from each other, a simulation of the experimental spectrum was undertaken to verify the correct assignment of the constants. The values for

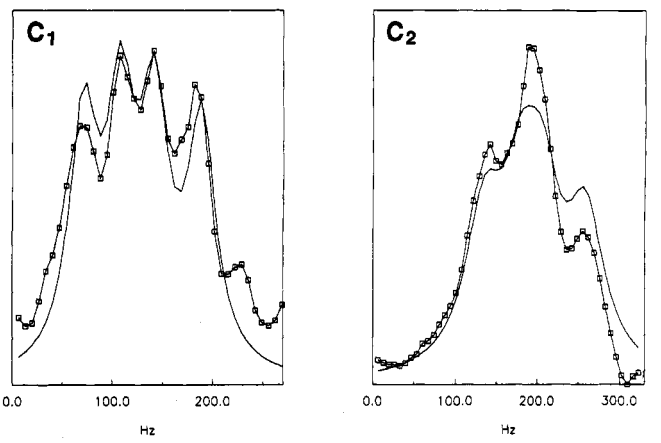

FIGURE 2: Simulation of the ^{13}C-spectrum of Figure 1. The experimental data were fit with a Lorentzian lineshape equation using a simplex algorithm. The fitting parameters agreed with the experimental values for the three coupling constants: C_1–C_2, C_1–C_3, and C_2–C_3 equal to 70, 40, and 45 Hz, respectively, and a line width of 33 Hz. The small discripancy between the theoretical curve and the spectrum is due to the presence of a Gaussian contribution to the line shape which is not accounted for in the fitting equation.

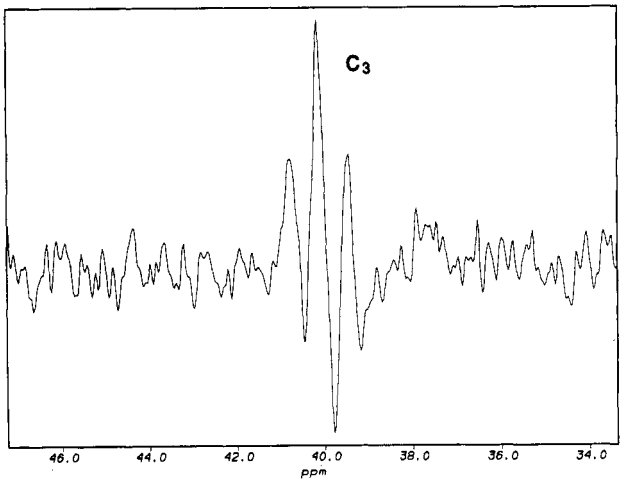

FIGURE 3: ^{13}C 1D-INADEQUATE (125.67 MHz) of the sample described in the legend of Figure 1 with ^{1}H-broadband decoupling using WALTZ-16 during evolution and ^{1}H-homodecoupling using MREV-8. The delay required for the generation of the double quantum coherence (τ) was optimized for a coupling of 50 Hz.

the coupling constants are 70, 40, and 45 Hz for C_1–C_2, C_1–C_3 and C_2–C_3, respectively. Since the C_3 resonance is broadened by two strong ^{1}H–^{13}C dipolar interactions, additional measurement of coupling constants from this multiplet is prohibited. Any such measurements would, however be redundant.

For the measurement of the remaining carbon–proton coupling constants, C_3–H_{3a} and C_3–H_{3e}, a 1D-INADEQUATE ^{13}C-NMR experiment was performed (Figure 3). Note that this is very effective in eliminating the background from unlabeled lipid seen in Figure 1. ^{1}H-heterodecoupling was accomplished using WALTZ-16 during evolution and ^{1}H-homodecoupling was accomplished using MREV-8 during acquisition. The latter is intended to remove the large ^{1}H–^{1}H coupling while retaining a scaled coupling for each ^{13}C–^{1}H pair (Webb & Zilm, 1989). Two couplings of 85 Hz were observed with this experiment before correction with the scaling factor. An experimental scaling factor of 0.51, which is close to the theoretical value of 0.54, was measured by comparing the $^{13}C_1$–^{1}H (anomeric carbon) coupling of a fully ^{1}H-coupled ^{13}C-NMR spectrum of a sulfolipid (data not shown) with a

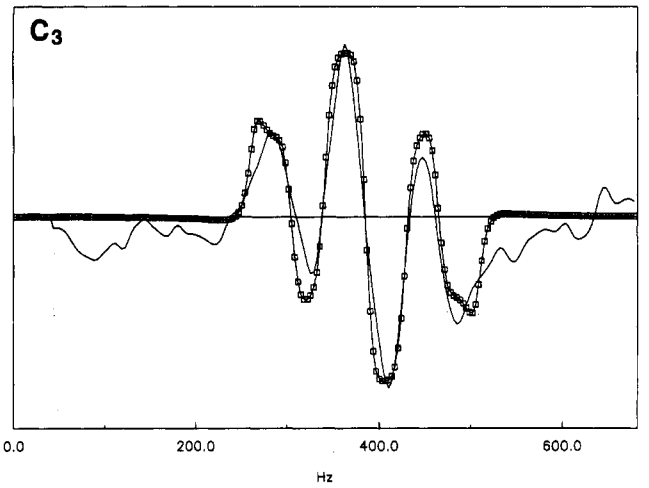

FIGURE 4: The experiment described in Figure 3 was simulated with a C program which calculates a theoretical spectrum resulting from the 1D-INADEQUATE pulse sequence (90-τ-180-τ-90-acq) using a density matrix formalism. The theoretical parameters $^1J_{C3-Ha}$ and $^1J_{C3-Ha}$ that best fit the experimental spectrum are both equal to 85 Hz.

^{1}H-homodecoupled spectrum collected under similar conditions. Since the antiphase character of the signals arising from the 1D-INADEQUATE experiment may lead to unexpected cancelation of some parts of a resonance, this experiment was simulated to ensure a correct measurement of the splittings from the NMR data. The details of the simulation are given in the legend of Figure 4.

Determination of the Spin of the Dipolar Couplings. Because expression 1 can lead to either a positive or a negative dipolar contribution it is important to measure the sign of the splitting in spectra such as those shown in Figures 1–3. It is also important to separate scalar contributions which are large for directly bonded spin pairs. As discussed elsewhere (Sanders & Prestegard 1991, 1992; Aubin & Prestegard, 1993) motional averaging scales the dipolar portion of the couplings but not the scalar part. Varying the overall order of the DMPC/CHAPSO system, thus, provides a way to extract the sign of dipolar couplings. Temperature was previously used to vary the degree of order (Aubin & Prestegard, 1993). Here again, lowering the temperature produces a gradual transition from an ordered to an isotropic phase. Figure 5 shows a series of ^{13}C-NMR spectra for the C_2 carbon of G_{M3} in a DMPC/CHAPSO 3:1, 35% (w/w) lipid system as a function of temperature. The C_2 resonance gradually loses its triplet-like multiplicity to show a doublet at 27.4 °C suggesting that only one of the dipolar couplings, $D_{C1,C2}$ or $D_{C2,C3}$ cancels its scalar part, $^1J_{C1,C2}$ or $^1J_{C2,C3}$. Thus one dipolar coupling must have a negative sign and the other a positive sign. Also C_1 undergoes a significant upfield shift of 4.5 ppm between 40 °C and 20 °C. This shift restricts the possible geometries of the carboxyl group in the sialic acid fragment.

The dipolar contributions were extracted from the measured couplings by correcting them using scalar couplings of 70, 40, and 133 Hz for C_1–C_2, C_2–C_3 and C_3–$H_{3a,e}$, respectively. Unfortunately, the temperature variation experiment was not able to distinguish which dipolar coupling, namely $D_{C1,C2}$ or $D_{C2,C3}$, is negative. Also, we were unable to evaluate the sign of the ^{13}C–^{1}H dipolar couplings leaving a total of three unknowns. However, it is a reasonable assumption to give both C_1–C_2 and C_3–H_{3a} couplings the same sign since the crystal structure of sialic acid used to obtain the molecular coordinates (O'Connel, 1973) shows that the corresponding vectors are nearly parallel. Thus, there are four possible sets

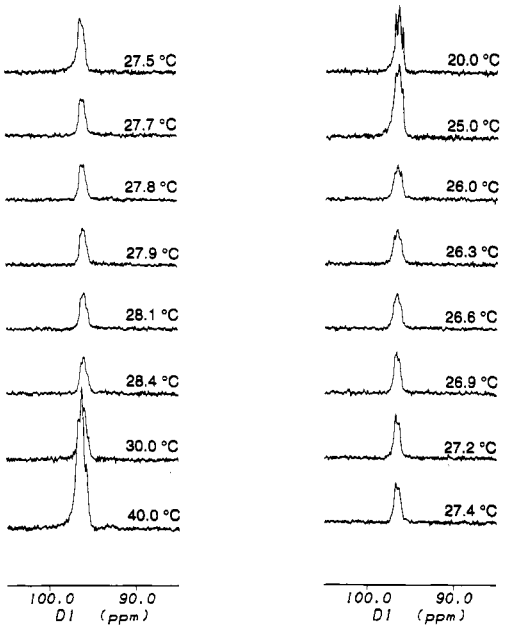

FIGURE 5: ^{1}H-decoupled inverse-gated ^{13}C-NMR spectrum (125.67 MHz) of the sample described in the legend of Figure 1 recorded at variable temperature.

Table I: Dipolar Couplings Measured from ^{13}C-NMR Spectra of G_{M3} Dissolved in a DMPC/CHAPSO (3:1) System at 40 °C

	observed	predicted
C_1–C_2	0 ± 15 Hz	6 ± 15 Hz
C_1–C_3	−85 ± 15 Hz	85 ± 15 Hz
C_2–C_3	40 ± 15 Hz	41 ± 15 Hz
C_3–H_{3a}	23 ± 40 Hz	10 ± 40 Hz
C_3–H_{3e}	−289 ± 40 Hz	−305 ± 40 Hz
δ_{COO}	−4.5 ppm	−2.2 or −4 ppm[a]

[a] Depending on the rotameric state of the carboxyl group (see text).

of signs for dipolar couplings among directly bonded spin pairs: (+,−,+,+); (+,−,−,+); (−,+,+,−) and (−,+,−,−) for $D_{C1,C2}$, $D_{C2,C3}$, $D_{C3,H3e}$ and $D_{C3,H3a}$, respectively. In the case of our nonbonded coupling, C_1–C_3, no scalar coupling was resolved. Thus, this observed coupling is purely dipolar. Since its magnitude does not change with the assumed sign it was handled in our program as an absolute value. One set of dipolar coupling input is summarized in Table I.

Analysis of Dipolar Couplings. An order matrix analysis was performed for each set of couplings using a program previously described (Aubin & Prestegard, 1993). A search was conducted in two stages using criteria for allowed solutions which were based on differences between predicted and measured couplings. Initially, the program searched the whole space of the order matrix by incrementing the five order parameters with steps of 0.03 and allowing an experimental error equal to a full line width. The preliminary solutions obtained from this coarse search allowed the localization of regions where acceptable solutions could be found. The search was then repeated using smaller increments of 0.01 and a deviation between predicted and observed splittings of one-half a line width. From the four input sets, only two converged to acceptable solutions. These sets correspond to sets 3 and 4. In set 3, the C_1–C_2 and C_3–H_{3a} couplings are positive, the C_2–C_3 coupling is negative, and the C_3–H_{3e} coupling is negative. In set 4 the C_1–C_2 and C_3–H_{3a} couplings are positive, the C_2–C_3 coupling is negative, and the C_3–H_{3e} coupling is positive. The various principal order parameters (S_{XX}, S_{YY}, and S_{ZZ}) and the eigenvectors expressing the average orien-

Table II: Order Parameters and Direction Cosines from the Order Matrix Analysis of the Couplings in Table I

order parameters	direction cosines		
	x	y	z
set 3			
S_{XX} –0.25	–0.352	0.936	–0.006
S_{YY} –0.48	0.822	0.312	0.476
S_{ZZ} 0.73	0.447	0.163	–0.880
set 4			
S_{XX} –0.26	–0.349	0.937	–0.019
S_{YY} –0.43	0.816	0.313	0.487
S_{ZZ} 0.69	0.462	0.155	–0.873

tation of the sialic acid ring in terms of the order frame, are strikingly similar for the best fit for each set (see Table II): they both give about the same average orientation with a high degree of order. The sialic acid orientation relative to the bilayer normal (Z axis) from the best fit of set 3 is represented in Figure 6. Actually we cannot differentiate between structures which are inverted with respect to the Z axis so we must keep this in mind as we build viable models for a G_{M3} headgroup structure.

The 5 pieces of data used in the above calculations are really minimal for the determination of orientation and order. It is therefore best to view results as a group of structures that are consistent with the experimental measurements within half a line width. To assess the degree of correlation between parameters in the allowed solutions, the Euler angles are plotted in Figure 7 for set 3 where the solution with the lowest rms deviation is represented by crosshairs. The distribution of the β and γ angles (○) is very narrow while that for the α angle (□) is a little more spread. Five solutions lie well outside the region containing the lowest rms deviation solutions (box b). We cannot totally discount these solutions, despite the fact that they do have a larger rms deviation (2%) as opposed to 0.3% for the best fit to set 3. They correspond to a negative value as opposed to a positive value for the nonbonded C_1–C_3 dipolar coupling. This emphasizes the importance of developing other methods of extracting sign information for dipole coupled pairs (J. Tolman and J. H. Prestegard, manuscript in preparation). A measure of motional asymmetry is given by the parameters η defined as $(S_{XX} - S_{YY})/S_{ZZ}$. Figure 8 shows a plot of η vs S_{ZZ} for set 3. The cross again indicates the best solution. This has a larger order parameter (0.73) and a lower asymmetry parameter (0.32) than observed previously for α-dodecyl sialyloside (S_{ZZ} = 0.4, η = 0.4).

Chemical shift anisotropy predictions based on the above order tensor elements and structural factors could in principle add confidence to our analysis. Unfortunately a rotational isomer of the carboxyl group on the sialic acid ring must be chosen. Chemical shifts of –2.2 ppm for a freely rotating carboxyl group or values varying from 8.5 ppm to –13.0 ppm are predicted depending on the rotameric state. A value of –4.5 ppm is measured and would correspond to an average torsion angle of 120 ± 45° for $O_{carboxyl}$–C_1–C_2–O_{ring}. This rotamer corresponds to a rotation of 90° along the C_1–C_2 bond when compared to the rotamer described in the crystal structure of β-*O*-methylsialic acid methyl ester (O'Connel, 1973). Our sialic acid is, however, α, and a rotamer similar to the one predicted is observed in another α sialic acid-containing crystal (Wright, 1990).

Interaction of Ca^{2+} with G_{M3}. Several observations have shown that a number of biological events involving G_{M3} require Ca^{2+} as a cofactor. In order to investigate the effect of Ca^{2+} binding on the structure and dynamics of G_{M3} an acid–base titration of the sialic acid in a DMPC/CHAPSO was first carried out to ascertain that the carboxylate was fully ionized. A pronounced upfield shift of the C_1 carbon resonance relative to the corresponding resonance in α-dodecyl sialyloside at pH 7 and slight downfield shift of the C_1 resonance of G_{M3} as the pH approached 7.0 suggests that the carboxyl group of G_{M3} is at least partially ionized at pH 7. Ca^{2+} was then added, in the form of $CaCl_2$, to a sample containing 10 mg of labeled G_{M3} dissolved in a mixture of 149 mg of DMPC/CHAPSO (3:1) in 0.300 mL of D_2O. This yields a ratio Ca^{2+}/G_{M3} of 2:1 and corresponds to a concentration of 69 mM which is higher than the range believed to be physiologically relevant. Given that binding constants as high as 100 M^{-1} have been determined for Ca^{2+} binding gangliosides (McDaniel & McLaughlin, 1985), one might have expected a complex to form. The ^{13}C-NMR spectrum of G_{M3}, however, remained unchanged; neither a shift for the resonances of the three labeled carbons nor any effect on the size of the coupling constants was observed. In an attempt to saturate the ganglioside environment with Ca^{2+} the concentration was increased to 280 mM. The C_1–C_2 coupling was reduced by 18 Hz under these conditions while the other two couplings did not experience any observable change. The magnitude of this change is too small to be characterized quantitatively, but since not all couplings scale proportionately, it clearly indicates a small but significant perturbation of the average orientation. It is also noteworthy that the resonance at 167 ppm coming from the acyl carbonyl linked to the sn-1 oxygen of the glycerol backbone of the DMPC molecule is shifted downfield by 0.35 ppm. This observation indicates a perturbation of the discoidal particles in the liquid crystal (Sanders

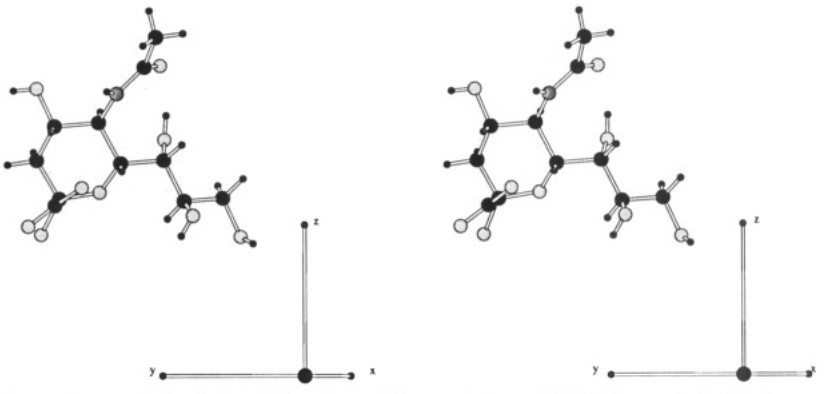

FIGURE 6: Stereoviews of the structure of the sialic acid moiety of G_{M3}; solution with 0.3% rms deviation from set 3. The conformation of the glycerol side chain and the acetamido group is taken from the crystal structure of β-*O*-methyl-*N*-acetylsialic acid methyl ester (O'Connel, 1973).

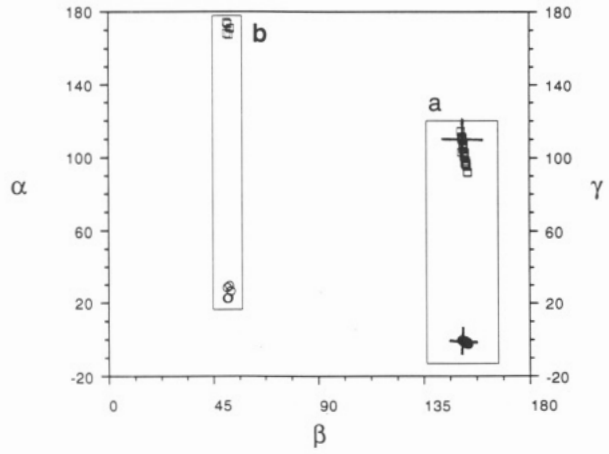

FIGURE 7: Euler angles for set 3 describing the order frame in terms of the molecular axis frame coordinates. β represents the angle between the z molecular axis and the Z order frame axis; α and γ represent rotations along the Z and z axes; respectively. (□): β vs α, and (○): β vs γ. The crosses indicate the solution with 0.3% rms deviation.

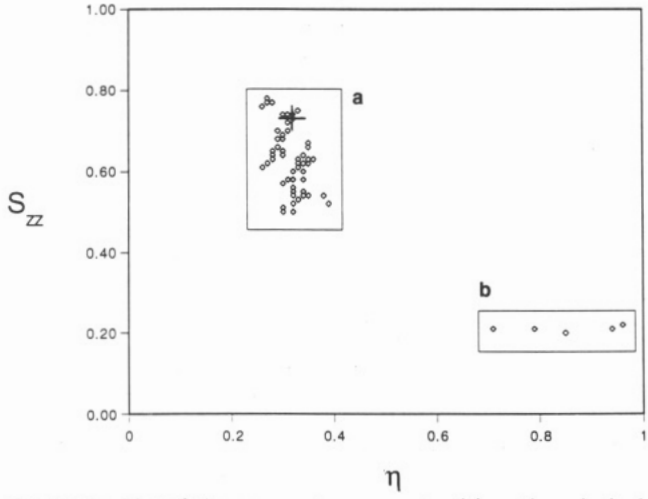

FIGURE 8: Plot of the asymmetry parameter (η) vs the principal order parameter (S_{ZZ}) for set 3.

& Prestegard, 1990); a similar observation has been reported previously (Frenske *et al.*, 1991). The small perturbation of the G_{M3} structure may indicate either a smaller than expected binding constant or the rather free accessibility of the carboxyl group in the native conformation.

Interaction of Wheat Germ Agglutinin with G_{M3}. Wheat germ agglutinin is known to interact with derivatives of G_{M3}, and one might expect some alteration of the average order or conformation upon binding of this protein. Figure 9 shows two ^{1}H-decoupled ^{13}C-NMR spectra of G_{M3} (2 mg) dissolved in a DMPC/CHAPSO system in a Tris-HCl buffer in D_2O at pH 7.4 containing 0.1 M NaCl and 0.01 M $CaCl_2$ at 40 °C. The bottom trace is a reference spectrum and the top trace shows a specific broadening of the C_1, C_2, and C_3 resonances upon addition of 12 mg of WGA corresponding to 67% occupation of binding sites (note that there are four binding sites per dimer). Addition to just half this level showed approximately half the broadening, and addition of free *N*-acetylglucosamine as a competitor to a level of NAcGlc/G_{M3} ratio of 2:1 completely reversed the broadening. These observations present clear evidence that, under the conditions of the study, WGA interacts with the sialic acid moiety of G_{M3}. We also know that the exchange between free and bound states is rapid on the NMR time scale. We do not know the actual extent of binding from the experiments presented, but

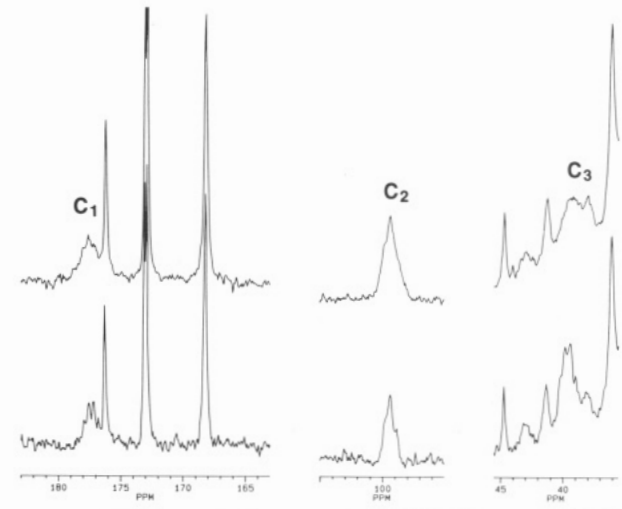

FIGURE 9: ^{1}H-decoupled inverse-gated ^{13}C-NMR spectra (125.67 MHz) of 2 mg of [^{13}C]G_{M3} dissolved in a DMPC/CHAPSO (3:1) system in Tris-HCl buffer at pH 7.4 containing NaCl (0.1M) and $CaCl_2$ (0.01M) recorded at 40 °C. The bottom trace is a reference spectrum; top trace shows a spectrum recorded with 12 mg of WGA corresponding to a G_{M3}/binding site ratio of 67%. Note the specific broadening of C_1, C_2, and C_3.

Table III: Angular Deviation between Membrane-Oriented Sialic Acid Residue of G_{M3} Shown in Figure 6 and the Six Low-Energy Conformers of G_{M3} in Solution Reported by Siebert *et al.* (1992)

model[a]	θ, deg
a (I, A)	65
b (I, B)	79
c (II, A)	55
d (II, B)	44
e (III, A)	58
f (III, B)	85

[a] The letters a–f correspond to the six combinations of torsion angles from the two glycosidic bonds: NeuAc-α-(2,3)-Gal (I: −165°, −25°; II: −78°, 19°; and III: 84°, 34°) and Gal-β-(1,4)-Glc (A: 51°, 1° and B: 5°, −49°).

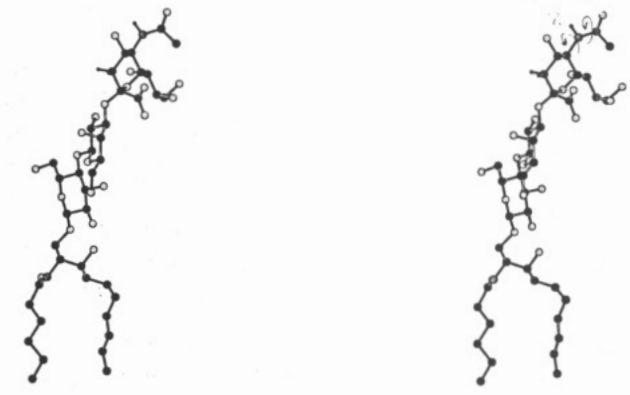

FIGURE 10: Stereoview of G_{M3} modeled from the result shown in Figure 6 (see text for details).

based on a free sialic acid binding constant of 200 M^{-1} (Kronnis & Carver, 1985) we would expect approximately 32% of G_{M3} to be bound. Despite this expectation, no significant changes in splitting or changes in the chemical shift of the carboxyl group are observed.

DISCUSSION

The orientational and motional description derived from the NMR data presented above is limited to the pyranose ring of sialic acid. Even the orientation of the glycerol side chain and the acetyl group of sialic acid presented in Figure 6 is not

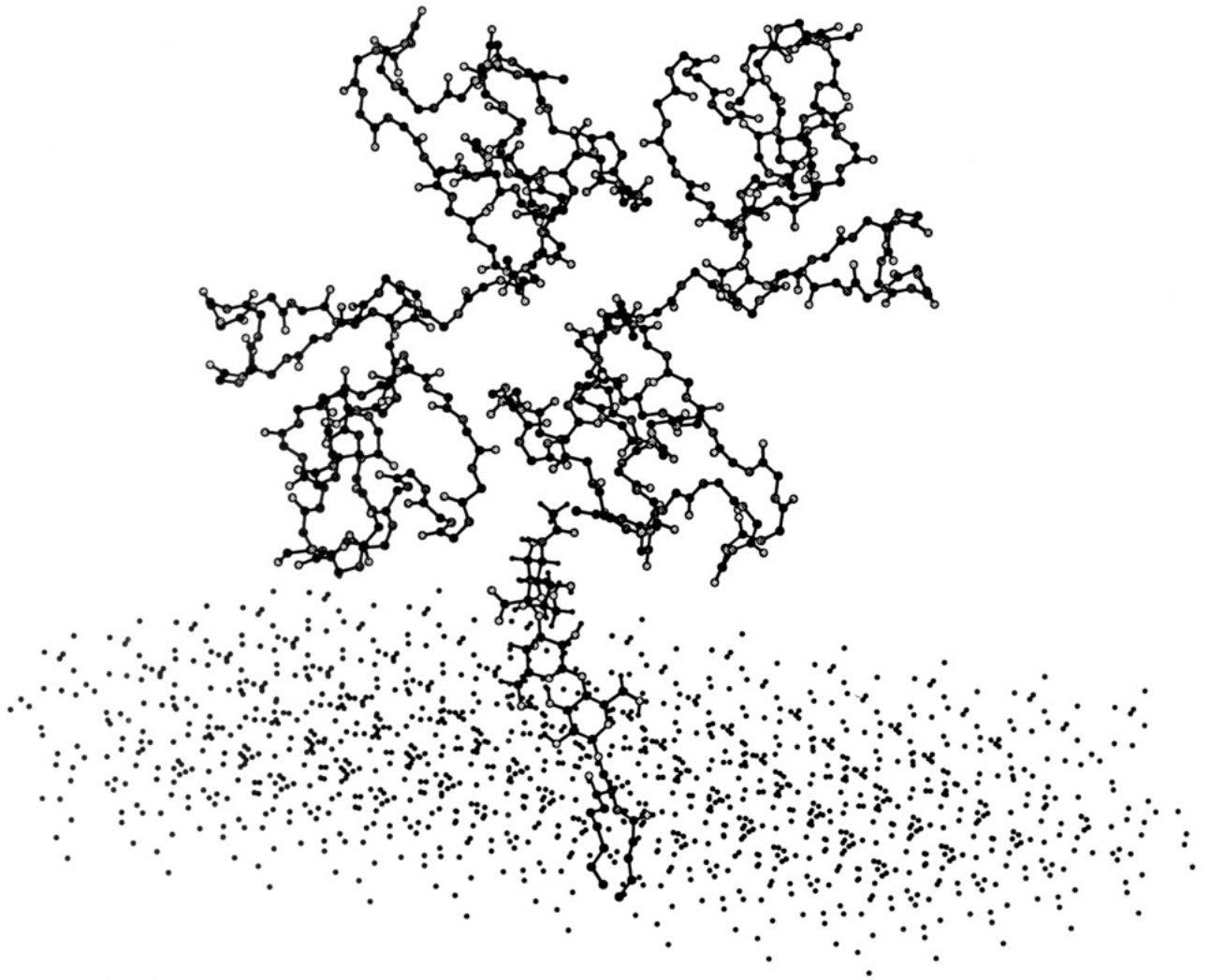

FIGURE 11: Model of the interaction between WGA and the sialic acid residue on G_{M3}. The monolayer was constructed from the data reported by Pearsun and Pasher (Pearsun & Pasher, 1979) where the alkyl chains were truncated for sake of clarity. Since, the ceramide backbone of G_{M3} and the glycerol portion of DMPC are almost isostructural, these two moieties were overlaid in order to ensure a correct positioning of the headgroup in respect to the membrane surface. The sialic acid moiety of G_{M3} was overlaid with its counterpart in the crystal so as to dock the headgroup in the binding site.

determined but is taken from the crystal structure of sialic acid (O'Connel, 1973). Information about the six torsion angles connecting the sialic acid to the ceramide backbone cannot be obtained directly. However, as shown below, a structure of G_{M3} ganglioside in a bilayer system consistent with the orientation of sialic acid reported in this study can be constructed by using literature data on similar systems.

Solution structures of G_{M3} determined by a combination of high-resolution NMR techniques and hard-sphere exo-anomeric calculations suggested that the headgroup of G_{M3} in a micellar system shares a conformational behavior with the cleaved headgroup in aqueous solution (Siebert *et al.*, 1992). Six low-energy conformers for the headgroup were generated from calculations on the system using NOE constraints. It is at first reasonable to screen these structures for consistency with our observations. The addition of a ceramide moiety to the above structures and modeling of the orientation of the attached glucose moiety can be accomplished using data on glucose-terminated glycolipids which have been studied in membrane-like environments (Jarrell *et al.*, 1987; Skarjune & Oldfield, 1982).

The coordinates of the crystal structure of galactosyl ceramide reported by Pascher and Sundell (Pascher & Sundell, 1977) were used as a starting point for the above modeling. The orientation of the glucose residue of G_{M3} headgroup at the membrane surface is based on structural data obtained from ^{2}H-NMR studies of 1,2-di-*O*-tetradecyl-3-*O*-(β-D-glucopyranosyl)glycerol (DTGL) (Jarrell *et al.*, 1987) and glucosylceramide (Skarjune & Oldfield, 1982) in a bilayer membrane system. The glucose ceramide glycosidic bond was adjusted with the following torsion angles $\phi = 13°$; $\psi = 173°$ which correspond to the most reasonable structure of DTGL according to Jarrell *et al.*, and the O–C_1–C_2–N dihedral angle in the ceramide backbone was manually adjusted to 177 °C to allow the orientation to approximate the structure determined by Skarjune and Oldfield for glucosyl ceramide. Note that the orientation of the glucose moiety reported by Jarrell *et al.* is very similar to the structure from the Oldfield data (a difference of 10 °C between an axis that passes through C_1 and C_4 in both compounds). Six G_{M3} models were then derived by overlaying the glucose ring in the membrane anchored glucosylceramide and the solution structures of the G_{M3} headgroup. Assuming the ceramide alkyl chains lie along the bilayer normal, the sialic acid moiety orientation in each structure can now be examined for consistency with our data. To better assess the degree of mismatch between the models and the sialic acid orientation depicted in Figure 6, direction cosines between our experimentally determined principal order

axis and a corresponding residue fixed axis in each of the six structures were calculated. The resulting angles of deviation are presented in Table III. All angles have been converted to ones less than 90° because we cannot distinguish structures with an inverted Z axis. No model matches our orientation very well. However, structure **d** presents the smallest deivation (44°). Moreover, modest manipulation of the four torsion angles of the headgroup glycosidic bond (<30 ° each) led to a perfect match. This structure is depicted in Figure 10.

The reasons for the mismatch of our orientation to any of the solution models could be many. First, it is possible that our particular membrane-like environment induces significant conformational changes in the headgroup. We have documented similar effects for an alkyl glucoside and Jarrell and co-workers have documented such an effect for sialylglycerolipids (Frenske *et al.*, 1991). It is also possible that the differences are due to motional averaging effects. We do observe a motionally averaged structure, not a discrete form. A relatively high-order parameter (0.73), however, suggests these averaging effects would not be large. Despite differences, both model d and the adjusted structure display reasonably well-extended headgroups. The latter point is of considerable interest; on the basis of HSEA calculations, it has been proposed (Kaizu *et al.*, 1986; Hakomori, 1986) that the headgroup of G_{M3} adopts an overall orientation where the carbohydrate axis is perpendicular to the ceramide axis. Model d would appear to disagree with these predictions.

Perturbations of the structure depicted in Figure 10 by either the addition of divalent ions (Ca^{2+}) or WGA appear to be small. In part, insensitivity to factors such as this may be connected with the apparent rigidity. Order parameters in the range of 0.5–0.8 are higher than those for our previous structures of α-dodecyl sialyloside (0.4) and alkyl glucoside (0.35). However, both of these have mobile, single-chain anchors as opposed to a ceramide which has two. Works on lipids with double-chain anchors, for example, those of Jarrell (Renou *et al.*, 1989) on ditetradecyl lactoside do give higher order parameters (0.52). While it may still be somewhat surprising that the addition of an extra glycosidic linkage generates so little additional motional freedom, this is not unprecedented. The terminal galactose residue in GM_1 has been shown to exhibit substantial motional restriction as well (Jarrell *et al.*, 1992).

The definite interaction of WGA with G_{M3} and the small corresponding structural perturbation would require that the binding site in WGA be configured so that binding could occur without significant penetration of parts of the protein into the bilayer surface. The crystal structure of the WGA–sialyl–lactose complex at 2.2 Å resolution reported by Wright (Wright, 1990) was used to examine possibilities for unfavorable membrane–protein interactions. The molecular coordinates were imported from the Protein Data Bank structure 1WGC and binding sites generated by translation of appropriate subunits in the unit cell. The protein contains four domains (ABCD) that dimerize to form the active species. Four binding sites are located between domains on two different polypeptide chains, two at BC contacts and two at AD contacts.

Figure 11 shows a model of WGA–G_{M3} interaction at the membrane surface. For the sake of clarity, only the BC domains are shown. The structure represented in Figure 10 was inserted in a monolayer of 45 DMPC molecules built from the data of Pearson and Pasher (Pearson & Pasher, 1979). The glycolipid was buried at a level which places the ceramide backbone in the plane of the glycerol units and the sialic acid rings of G_{M3} and the WGA–sialyl–lactose complex were overlaid. The details of the model are given in the legend of Figure 11. The model does not show any unfavorable interactions between the protein and the membrane surface which suggests that the G_{M3} headgroup in the conformation we favor presents its sialic acid moiety in the proper orientation for interaction with the protein. The remaining AD domains, not represented in Figure 11, would position next to the BC domains to form a cube-like structure. The orientation of the additional binding sites would be very similar.

Thus, we have been able to determine a probable membrane-bound conformation for an important sialic acid terminated glycolipid, and we have been able to examine perturbations to this structure on binding of a protein known to mediate cell agglutination. The methodology relies heavily on recently perfected methods for enzymatically attaching sialic acid residues which are enriched in ^{13}C and the observation of these sites by oriented sample NMR methods. The methodology is easily extended to a variety of sialic acid containing, membrane-anchored molecules. We anticipate additional data which may allow generalizations about the nature of protein-carbohydrate interactions that occur at membrane surfaces.

ACKNOWLEDGMENT

Dr. Julian Tirado-Rives is gratefully acknowledged for providing the software MindTool used for the generation of Figures 6 and 10 and the FIT program used for the simulation of the ^{13}C spectrum of Figure 2. Michael Andrec is acknowledged for his help in the simulation of the 1D-INADEQUATE.

REFERENCES

Aubin, Y., & Prestegard, J. H., (1993) *Biochemistry 32*, 3422–3428 and references cited therein.
Bax, A., Freeman, R., & Frenkiel, T. A. (1981) *J. Am. Chem. Soc. 103*, 2102–2104.
Frenske, D. B., Lettellier, M., Roy, R., Smith, I. C. P., & Jarrell, H. C. (1991) *Biochemistry 30*, 10542–10550 and references cited therein.
Grayson, G., & Ladisch, S. (1992) *Cell. Immunol. 139*, 18–29.
Hakomori, S.; (1981) *Annu. Rev. Biochem. 50*, 733–764.
Hakomori, S., & Kannagi, R. (1983) *J. Natl. Cancer Inst. 71*, 231–251.
Hakomori, S. (1986) *Sci. Am. 254*, 44–53.
Hanai, N., Nores, G. A., MacLoed, C., Torres-Mendez, C.-R., & Hakomori, S. (1988) *J. Biol. Chem. 262*, 10915–10921.
Hanai, N., Nores, G. A., & Hakomori, S. (1988) *J. Biol. Chem. 262*, 6296–6301.
Ichikawa, Y., Look, G. C., & Wong, C.-H. (1992) *Anal. Biochem. 202*, 251.
Ito, Y., & Paulson, J. C. (1993) *J. Am. Chem. Soc. 115*, 1603–1605.
Iwamori, M., & Nagai, Y. (1978) *J. Biochem. 84*, 1609–1615.
Jarrell, H. C., Jovall, P. A., Giziewicz, J. B., Turner, L. A., & Smith, I. C. P. (1987) *Biochemistry 26*, 1805–1811.
Jarrell, H. C., Singh, D., & Grant, C. W. M. (1992) *Biochim. Biophys. Acta 1103*, 331–334.
Kaizu, T., Levery, S. B., Nudelman, E., Stemkamp, R. E., Hakomori, S. (1986) *J. Biol. Chem. 261*, 11254–11258.
Koerner, T. A. W., Prestegard, J. H., Demou, P. C., & Yu, R. K. (1983) *Biochemistry 22*, 2676–2687.
Kronnis, K. A., & Carver, J. P. (1985) *Biochemistry 24*, 826–833.
Lasky, L. A. (1992) *Science 258*, 964–969.
Lemieux, R. U. (1982) *IUPAC Frontiers of Chemistry*. (Lasidler, K. J., Ed.) pp 3–25, Pergamon Press, Oxford, U.K.
McDaniel, R., & McLaughlin, S. (1985) *Biophys. Biochem. Acta 819*, 153–160.
O'Connel, A. M. (1973) *Acta Crystallogr. B29*, 2320.

Pascher, I., & Sundell, S. (1977) *Chem. Phys. Lipids 20*, 175–191.
Pearson, R. H., & Pasher, I. (1979) *Nature 281*, 499–501.
Pines, A., Chang, J. J., & Griffin, R. G. (1974) *J. Chem. Phys. 61*, 1021–1030.
Ravindranath, M. H., Tsuchida, T., & Irie, R. F. (1989) in *Gangliosides and Cancer* (Oettgen, H. F., Ed.) pp 79–91, VHC Publishers, New York.
Rosenberg, A., & Schengrund, C.-L., Eds. (1976) *Biological Roles of Sialic Acid*, Plenum Press, New York.
Sanders, C. R., & Prestegard, J. H. (1990) *Biophys. J. 58*, 447–460.
Sanders, C. R., & Prestegard, J. H. (1991) *J. Am. Chem. Soc. 113*, 1987–1996.
Sander, C. R., & Prestegard, J. H. (1982) *J. Am. Chem. Soc. 114*, 7096–7107.
Schauer, R., Ed. (1983) *Sialic Acids*, Springer-Verlag, New York.
Sharon, N., & Halina, L. (1993) *Sci. Am.* January, 82–89 and references cited therein.
Siebert, H. C., Reuter, G., Schauer, R., Von der Lieth, C.-W., & Dabrowski, J. (1992) *Biochemistry 31*, 6962–6971.
Skarjune, R., & Oldfield, E. (1982) *Biochemistry 21*, 3154–3160.
Song, W., Vacca, M. F., Welti, R., & Rintoul, D. A. (1991) *J. Biol. Chem. 266*, 10174–10181.
Thurin, J., & Bechtel, B. (1989) in *Gangliosides and Cancer* (Oettgen, H. F., Ed.) pp 159–165, VHC Publishers, New York.
Webb, G. & Zilm, K. W. (1989) *J. Am. Chem. Soc. 111*, 2455–2463.
Wiegandt, H., Ed. (1985) *Glycolipids in New Comprehensive Biochemistry* (Neugerger, A., & van Deenan, L. L. M., Eds.), Vol. 10, p 199.
Wright, C. S. (1990) *J. Biol. Chem. 215*, 635–651 and references cited therein.